NEAR-FIELD CHIPLESS-RFID TAGS WITH SEQUENTIAL BIT READING IMPLEMENTED IN PLASTIC SUBSTRATES

Herrojo C.[1], Mata-Contreras J.[1], Paredes F.[1], Núñez A.[2], Ramon E.[2], Martín F.[1]

[1]CIMITEC, Departament d'Enginyeria Electrònica, Universitat Autònoma de Barcelona, 08193 Bellaterra, Barcelona, Spain
[2]Institut de Microelectrònica de Barcelona, IMB-CNM (CSIC), Bellaterra, Spain
E-mail: Ferran.Martin@uab.es

Abstract

Chipless radiofrequency identification (chipless-RFID) systems based on near-field coupling between the tag and the reader and sequential bit reading, with tags implemented on plastic substrates, are presented in this paper. In the proposed system, the tag is a set of identical resonant elements (S-shaped split ring resonators –S-SRRs), inkjet-printed on a plastic substrate (PEN), forming a resonator chain. The presence or absence of resonant elements at predefined and equidistant positions in the chain determines the logic state '1' and '0', respectively, associated with each resonant element. The reader is a coplanar waveguide (CPW) transmission line fed by a harmonic signal tuned to the resonance frequency of the resonant elements of the chain. Tag reading is achieved by displacing the chain of resonant elements above the CPW transmission line, in close proximity to it, so that near-field coupling between the CPW transmission line and the resonant elements of the tag results. By this means, the injected carrier signal is amplitude modulated, provided the transmission coefficient of the line varies with the presence or absence of resonant elements in the chain, and the identification (ID) code is contained in the envelope function. The functionality of the proposed system, with 10-bit tags occupying an area of 1.35 cm^2 (corresponding to an information density of 7.4 bit/cm^2), is demonstrated.

1. Introduction

Radiofrequency identification (RFID) is a wireless RF technology for the identification and tracking of items, consumer products, animals, vehicles, etc [1]. A typical RFID system is composed by the tag, which contains a unique ID code stored in a silicon integrated circuit (IC), or chip, and the reader. In passive RFID systems operating in the ultra-high-frequency (UHF) band, the tag and the reader are equipped with antennas for communications purposes through the far-field, and the reader provides also the necessary energy to power-up the tag. These passive UHF-RFID tags are relatively cheap, at least as compared to active tags (typically operating at microwave frequencies), exhibit high data capacity, and do not need to be at short distance to the reader for interrogation purposes. Thus, UHF-RFID systems are by far superior to identification systems based on optical barcodes in terms of data storage capability, and reading distance (line-of-sight is not required and read ranges of several meters can be achieved with the activation energy of currently available tag chips). However, the cost of UHF-RFID tags, dictated by the presence of the chip, is of the

order of several Eurocents, and this cost is too high for the penetration of the UHF-RFID technology in many applications where low-cost item products are involved.

To alleviate the cost of chiped tags, the chipless-RFID technology emerged several years ago [2-7]. In chipless-RFID tags, chips are replaced with printed encoders containing the ID code. Although the cost of these encoders can be potentially situated below the Eurocent barrier on account of the current cost of conductive inks, and future trends on the use of massive printing processes for tag fabrication (screen-printing, rotogravure, etc.), chipless tags have two main limitations, as compared to chip-based tags: (i) the data storage capability and (ii) the encoder size. Therefore the present challenges of researchers working on the topic of chipless-RFID are to reduce the size of the tags and to increase the number of bits as much as possible.

Chipless-RFID systems are based on two main approaches: (i) time domain based systems [8-17] and (ii) frequency domain based systems [2, 3, 18-37]. In chipless-RFID systems based on the former approach, tag reading is carried out through time domain reflectometry (TDR). TDR-based tags exhibit fast responses in comparison to frequency domain based tags. However, in TDR-based tags the tag ID is generated by the echoes of a pulsed signal caused by discontinuities or impedance mismatches in a delay line. In order to avoid overlapping of the reflected pulses, either large delay lines or very narrow pulses are needed. Hence, TDR-based tags exhibit a limited bit encoding capability. In frequency domain based chipless-RFID systems, encoders are implemented by means of resonant elements tuned at predefined frequencies. Such frequencies are distributed within a certain frequency band, and hence tag reading requires a multi-frequency interrogation signal covering the spectral bandwidth. Encoding is achieved by the presence or absence of abrupt spectral features in the amplitude, phase or group delay responses. In frequency domain based tags, each resonant element typically corresponds to 1 bit of information. However, tags based on multi-state resonators have been recently demonstrated [35-37] (in such tags, up to 2 bits per resonant element are achieved by resonator rotation). Finally, some chipless-RFID systems, designated as hybrid systems, use more than one domain (e.g. time, frequency, phase, polarization, etc.) simultaneously, in order to increase the number of bits per resonant element [28, 31-34].

Despite numerous efforts to increase the number of bits in the previous approaches, the reported chipless-RFID tags are far from the data capacity of chiped tags. The main limitation in frequency domain and hybrid based tags is the spectral bandwidth required to accommodate a large number of bits. This is related to the achievable information density per frequency (DPF), which is typically small due to the bandwidth occupied by each resonant element.

In [38], a novel time domain approach for the implementation of chipless-RFID systems, which potentially allows for unprecedented data capacities, was reported. In this approach, the tags are implemented by means of chains of identical resonators, all tuned to the same frequency. Encoding is achieved by the presence or absence of resonant elements at predefined and equidistant positions in the chain, and tag reading is carried out through near-field coupling. Namely, a transmission line is fed by a harmonic signal tuned to the resonance frequency of the tag resonators. By displacing the tag over the transmission line, in close proximity to it, magnetic coupling between the line and the tag arises provided a resonator lies on top of the line. Thus, line-to-resonator coupling is modulated by tag motion, and such modulation is controlled by

the tag ID. Such coupling modulation, in turn, modulates the transmission coefficient of the line and, consequently, the output signal is amplitude modulated as well. Therefore, the ID code is contained in the envelope function, and a simple envelope detector suffices for tag reading. Note that the spectral bandwidth is null (all the resonators are tuned to the same frequency) and hence the information DPF is virtually infinite. Hence, the number of bits is only limited by the area occupied by the resonators chain. In this paper, our aim is to demonstrate the functionality of this novel chipless-RFID approach with inkjet-printed tags on plastic substrates. This approach is of special interest in applications where the read distances can be sacrificed in favor of data capacity, such as security and authentication, where, typically, a large number of bits is necessary (e.g. secure paper in corporate documents, certificates, ballots, exams, etc.).

2. Principle of the proposed chipless-RFID system

The principle of operation of the proposed system is depicted in Fig. 1 [38]. The reader consists of a CPW transmission line fed by a harmonic signal, plus an envelope detector, preceded by a circulator, at the output port. The tags are implemented by means of S-SRR resonators (Fig. 2(a)) [39]. Such resonant elements are excited when they are situated on top of the CPW transmission line (in close proximity to it) as depicted in the figure, by virtue of the counter magnetic fields generated by the feeding signal [40]. However, in order to prevent from the coupling between the line and multiple resonant elements simultaneously, or between the resonant elements of the tag, an S-SRR has been etched in the back substrate side of the CPW transmission line, rotated 180º with regard to the S-SRRs of the tag chain (Fig. 2(b)). By this means, the resonance frequency of the pair of perfectly aligned S-SRRs (forming a broadside-coupled S-SRR) is smaller than the resonance frequency of a single S-SRR (4.4 GHz), and the above-cited couplings are prevented [41]. Indeed, the harmonic feeding signal is tuned to the fundamental resonance frequency of the broadside coupled S-SRR, f_0.

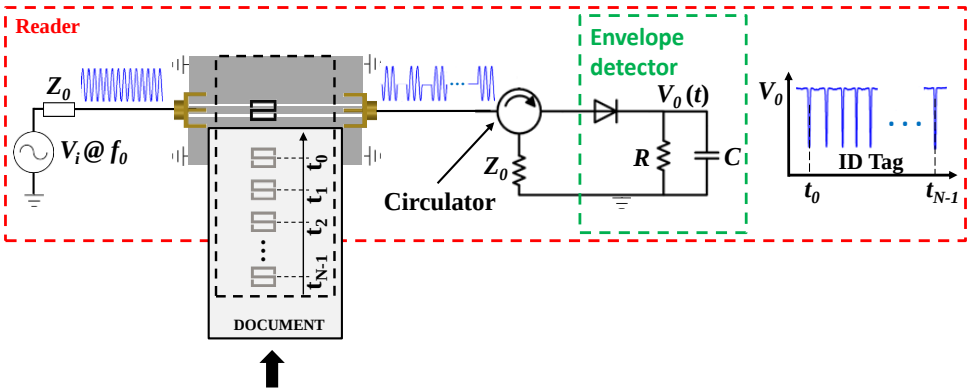

Fig. 1. Illustration of the working principle of the proposed chipless-RFID system.

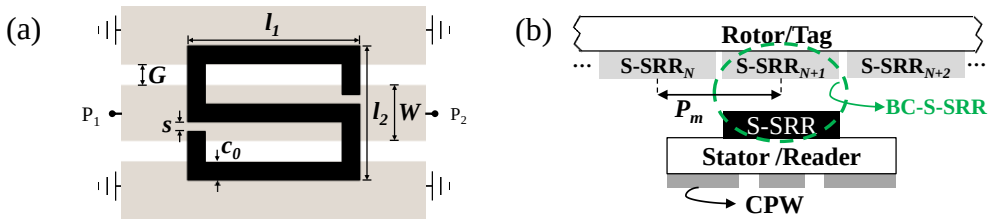

Fig. 2. S-SRR on top of a CPW (a) and cross sectional view of the S-SRR-loaded CPW and tag (b). Relevant dimensions are indicated.

Each time an S-SRR of the tag lies on top of the S-SRR of the line (logic state '1'), line-to-resonator coupling is maximized, and the transmission coefficient of the line at f_0 as well as the amplitude of the output signal is minimized. Conversely, if the S-SRR is not present in one of the predefined positions in the chain (logic state '0'), the modulus of the transmission coefficient is roughly 1, and the amplitude of the output signal is identical to the one of the input signal. Thus, tag motion effectively modulates the amplitude of the output signal, according to the ID code of the tag. Therefore, by extracting the envelope function, the ID code can be inferred. To this end, an envelope detector, implemented by means of a diode and low-pass filter, is used. Since the diode is a highly non-linear device, a circulator configured as an isolator is cascaded between the output port of the line and the envelope detector. By this means, unwanted mismatching reflections from the diode are avoided.

A key advantage of this approach, based on near-field coupling for tag reading, is the fact that the tag merely consists of a chain of resonant elements. Antennas are not needed, simplifying tag design, size, and cost. Alignment between the tag chain and the S-SRR of the line is required, but some tolerance is acceptable since the transmission coefficient of the line at the frequency of the broadside coupled S-SRR, f_0, is also significantly reduced when the S-SRR of the line and tag are not perfectly aligned. The air gap distance between the tag and the line has also influence on coupling modulation, since it varies the resonance frequency of the broadside coupled S-SRR, where maximum coupling arises. In practice, the frequency of the feeding signal should be set to a value slightly above f_0, the frequency of the broadside coupled S-SRR corresponding to the nominal air gap separation, since it is difficult to precisely control the air gap and to guarantee the invariability of it during tag motion. Note that if the frequency of the feeding signal is smaller than the resonance frequency of the broadside coupled S-SRR corresponding to a certain air gap separation, larger than the nominal, false readings may arise.

3. Substrate and ink characterization

In this paper, tags based on a chain of S-SRRs printed by inkjet on a plastic substrate are presented for the first time. The Polyethylene naphtalate (PEN) film (*Dupont Teijin Q65FA*) with thickness h = 125 μm was employed as flexible substrate. The dielectric constant and loss tangent of this material have been inferred by means of a split cylinder resonator (model *Agilent 85072A*). The resulting values have been found to be ε_r = 3.36 and $\tan\delta$ = 0.0042. Such loss tangent value is relatively small, not very far from the typical values of low-loss microwave substrates.

The used inkjet printer is the *Ceradrop Ceraprinter X-Serie*, and two layers of *DuPont™ PE410* conductive ink (with conductivity 7.28×10^6 S/m) have been printed in order to achieve a measured thickness of 3.3-3.5 μm.

4. Reader and tag design and fabrication

The CPW transmission line of the reader has been fabricated on the low-loss *Rogers RO3010* substrate with dielectric constant ε_r = 10.2, loss tangent $\tan\delta$ = 0.0022 and thickness h = 0.635 mm. Both the CPW layout and the pattern of the S-SRR of the

line have been achieved by means of a drilling machine (*LPKF H100*). The metal layer is copper with a thickness of 35 μm. The dimensions of the S-SRR, in reference to Fig. 2 are l_1 = 3.8 mm, l_2 = 2.96 mm, c_0 = 0.4 mm and s = 0.2 mm. With these dimensions, the resonance frequency of the broadside coupled S-SRR resulting by printing an identical S-SRR on the above cited plastic substrate, and by considering an air gap of 0.25 mm, is found to be f_0 = 4 GHz. The photograph of the fabricated S-SRR-loaded CPW is shown in Fig. 3(a).

In the tag, S-SRRs with dimensions identical to those of the S-SRR of the line must be used for coding purposes. The distance between adjacent S-SRRs (in case they are present in two adjacent predefined positions) is 0.2 mm, resulting in a chain period of 3.16 mm. This S-SRR separation is enough to avoid overlapping between adjacent resonant elements after the printing process. The photograph of the fabricated tag, with all bits set to '1', is depicted in Fig. 3(b).

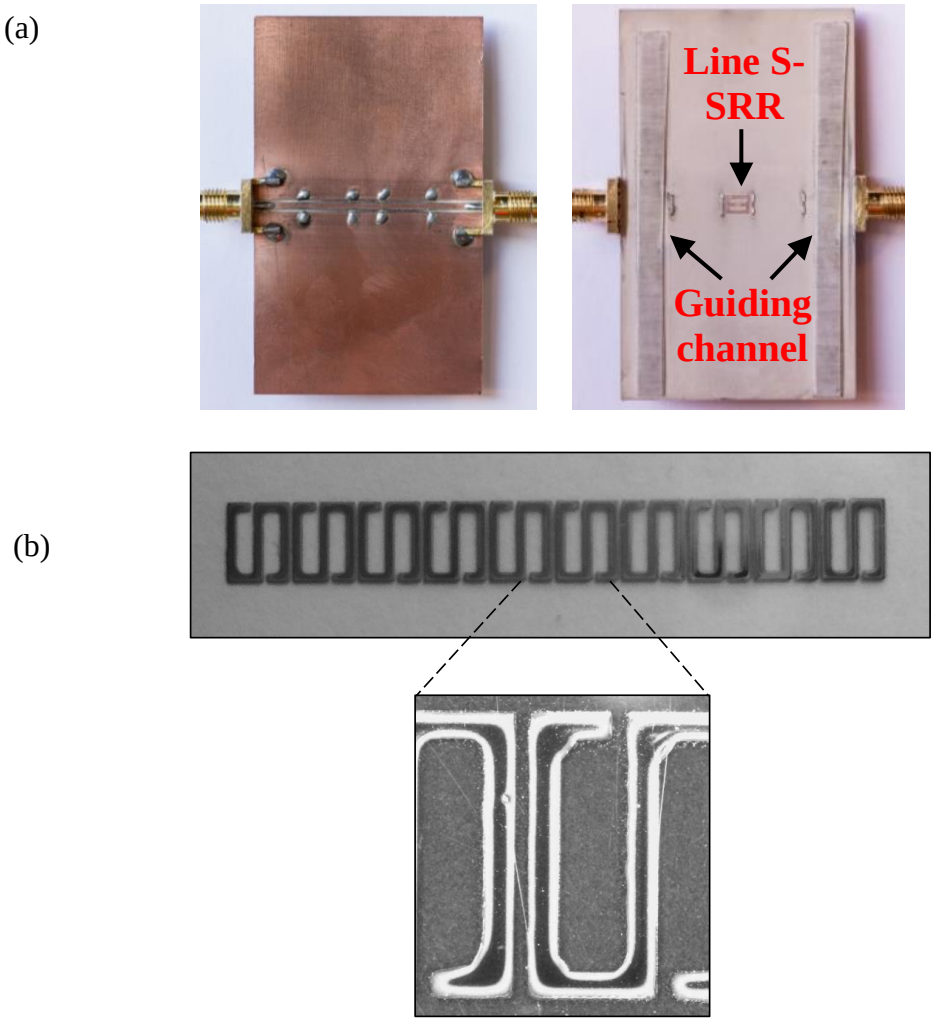

Fig. 3. Photograph of the fabricated S-SRR-loaded CPW used for reading purposes (a) and photograph of the fabricated 10-bit chipless-RFID tags (with code '1111111111') (b).

With regard to the additional elements necessary for a reading operation, the harmonic feeding signal is generated by means of the *Agilent E4438C* function generator. The envelope detector uses the *Avago HSMS-2860* Schottky diode and the

N2795A active probe (which acts as low-pass filter with R = 1 MΩ and C = 1 pF), connected to an oscilloscope (the *Agilent MSO-X-3104A*) in order to visualize the envelope function. Finally, the circulator is the *ATM ATc4-8*, operative in the frequency region of interest. The photograph of the experimental set-up is shown in Fig. 4.

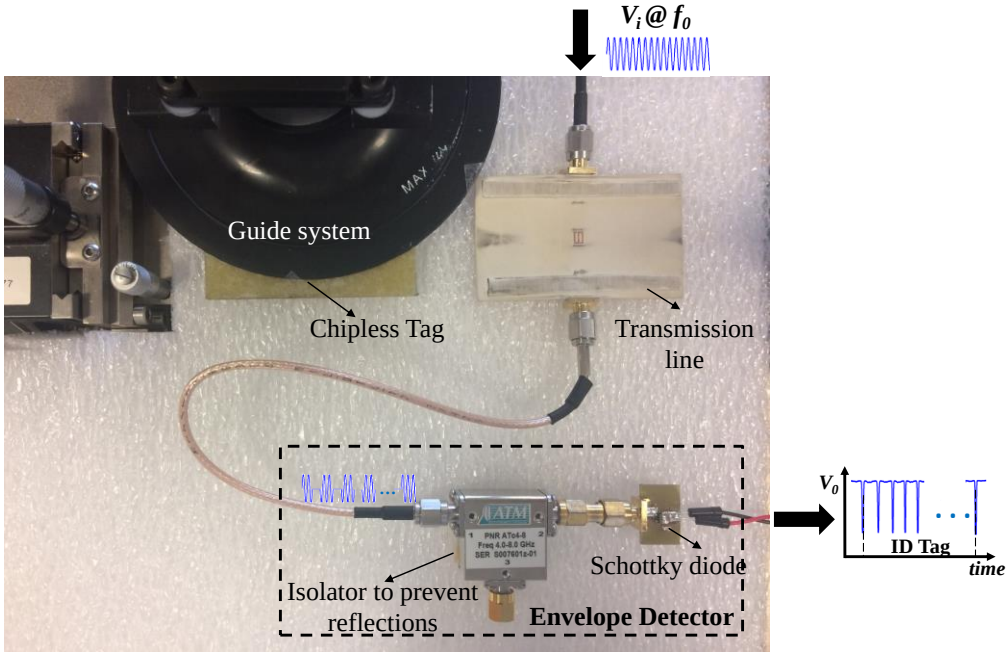

Fig. 4. Experimental set-up.

5. Results and discussion

The measured normalized envelope function corresponding to the tag of Fig. 3(b) is depicted in Fig. 5. Ten dips, corresponding to the ten S-SRRs, can be perfectly appreciated. Hence, the proposed chipless RFID system is validated by considering plastic substrates and resonant elements printed on it.

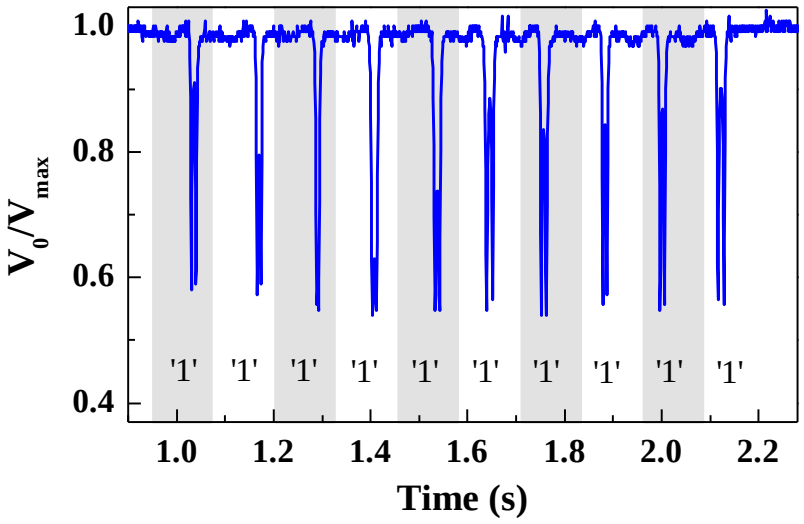

Fig. 5. Measured normalized envelope for the 10-bit chipless RFID tag of Fig.3 (b).

A detailed view of Fig. 5 indicates that in some cases a double dip, rather than a single dip, associated with the presence of a resonant element (‘1’ logic state) arises.

This is due to the fact that, in practice, it is very difficult to maintain the gap distance to the same value during tag motion. If the frequency of the feeding (carrier) signal is slightly above the frequency of the broadside coupled S-SRR (variable with the air gap), then two dips per resonant element are expected, as discussed in [42]. Nevertheless, the tag ID can be perfectly read provided the normalized amplitude of the envelope function is situated below a certain threshold (e.g. 0.8) when the resonant element associated with a certain bit is present in the tag.

Let us now discuss another important aspect, i.e., the possibility to program the ID code. To reduce fabrication costs, it is convenient to fabricate all identical tags, i.e., with all bits set to '1', and, in a later stage (writing operation), detune the necessary resonators to implement the required ID code. Detuning means to physical alter the resonators in order to shift their resonance frequency beyond the region of interest. By this means, a logic '0' state is associated to a detuned resonant element, equivalent to its absence in a predefined position of the chain. In practice, detuning can be achieved by cutting the resonant elements. Alternatively, by short-circuiting the terminals of the S-SRR one also expects a significant displacement of their resonance frequency. In this work, we have cut alternating S-SRRs in the tag of Fig. 3(b), corresponding to the ID code '1010101010'. The photograph of the programmed tag is depicted in Fig. 6, and its measured normalized envelope function is depicted in Fig. 7. The obtained envelope demonstrates that such programming approach works, on account of the obtained ID code. Beyond the proof-of-concept presented here, in a real scenario, detuning by means of laser ablation (cutting the resonant elements) or by means of inkjet printing (short-circuiting the terminals of the S-SRR) can be envisaged.

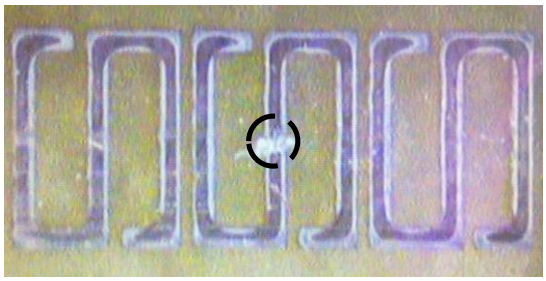

Fig. 6. Photograph of the programmed 10-bit tag, with alternating detuned S-SRRs.

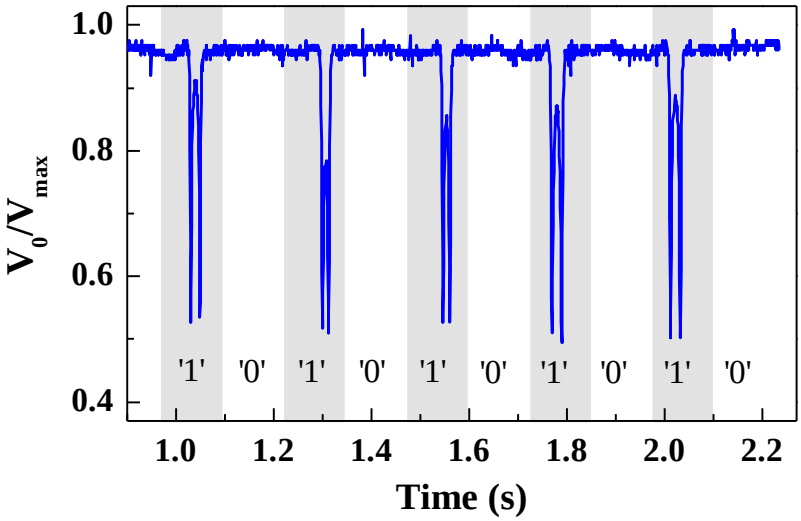

Fig. 7. Measured normalized envelope for the 10-bit chipless RFID tag of Fig. 6.

6. Conclusions

In conclusion, a chipless-RFID system based on near-field coupling between the tag and the reader and sequential bit reading has been validated by inkjet-printing the tags on a plastic substrate (PEN). Specifically, a 10-bit tag has been fabricated by using S-SRRs as resonant elements. By displacing the tag over the S-SRR-loaded CPW transmission line (active part of the reader) fed by a conveniently tuned harmonic signal, it has been demonstrated that the amplitude of the output signal is efficiently modulated according to the ID code of the tag. The experimental set-up implemented to extract the envelope function has revealed that the ID code is correctly obtained in the considered 10-bit chipless-RFID tags. The information density per area in the designed tags is 7.4 bit/cm^2. In the proposed system, the number of bits is only limited by the area occupied by the printed encoders (chain of resonant elements). Therefore, it is possible to obtain a number of bits comparable to that of chiped tags (96 bits, according to the EPC Class 1 Generation 2 Protocol), since 96 bits only require a S-SRR tag chain with 30.0 cm in length. This length is comparable with the dimensions of standard documents, and hence this approach can be useful for secure paper applications (e.g. for identification and authentication purposes). For such applications, the tags implemented on PEN can be conveniently laminated to embed them in paper substrates. Nevertheless, the next step in this research activity is to directly print the proposed chipless-RFID tags on conveniently functionalized paper. The possibility to program the tags by detuning the resonant elements has been also discussed, and a proof-of-concept, where the '0' state has been achieved by cutting the corresponding resonant elements, has been carried out.

Acknowledgements

This work was supported by MINECO-Spain (projects TEC2013-40600-R, TEC2016-75650-R and RTC-2014-2550-7), *Generalitat de Catalunya* (project 2014SGR-157), *Institució Catalana de Recerca i Estudis Avançats* (who awarded F. Martín), and by FEDER funds. C. Herrojo acknowledges MINECO for supporting his research activity through the FPI grant BES-2014-068164.

References

1. J. Landt, "The history of RFID", *IEEE Potentials*, vol. 24, pp. 8-11, 2005.
2. S. Preradovic and N. C. Karmakar, "Chipless RFID: bar code of the future," *IEEE Microwave Magazine*, vol. 11, pp. 87-97, 2010.
3. S. Preradovic and N. C. Karmakar, *Multiresonator-Based Chipless RFID: Barcode of the Future*, Springer, 2011.
4. N.C. Karmakar, R. Koswatta, P. Kalansuriya, R. E-Azim, *Chipless RFID Reader Architecture*, Artech House, 2013.
5. E. Perret, *Radio Frequency Identification and Sensors: From RFID to Chipless RFID*, John Wiley, New York, 2014.
6. R. Rezaiesarlak and M. Manteghi, *Chipless RFID: Design Procedure and Detection Techniques*, Springer, 2015.
7. N. C. Karmakar, M. Zomorrodi, C. Divarathne, *Advanced Chipless RFID*, John Wiley, Hoboken, NJ, 2016.
8. C. S. Hartmann, "A global SAW ID tag with large data capacity," in Proc. of *IEEE Ultrasonics Symposium*, October 2002, vol. 1, pp. 65–69.

9. A. Chamarti and K. Varahramyan, "Transmission delay line based ID generation circuit for RFID applications," *IEEE Microw. Wireless Compon. Lett.*, vol. 16, pp. 588-590, 2006.
10. M. Schüßler, C. Damm, and R. Jakoby, "Periodically LC loaded lines for RFID backscatter applications," in Proc. of *Metamaterials 2007*, Rome, Italy, October 2007, pp. 103-106.
11. N. Saldanha, D.C. Malocha, "Design Parameters for SAW multi-tone frequency coded reflectors" *2007 IEEE Ultrasonics Symp*., pp. 2087-2090, 2007.
12. M. Schüßler, C. Damm, M. Maasch, and R. Jakoby, "Performance evaluation of left-handed delay lines for RFID backscatter applications," in Proc. of the *IEEE MTT-S International Microwave Symposium 2008*, pp. 177-180.
13. S. Harma, V.P. Plessky, C.S. Hartmann, W. Steichen, "Z-path SAW RFID tag" *IEEE Trans. Ultrasonics, Ferroelectric Freq. Control*, vol. 55, pp. 208-213, 2008.
14. H. Tao, W. Weibiao, W. Haodong, S. Yongan, "Reflection and scattering characteristics of reflectors in SAW tags", *IEEE Trans. Ultrasonics, Ferroelectric Freq. Control*, vol. 55, pp. 1387-1390, 2008.
15. S. Harma, V.P. Plessky, L. Xianyi, P. Hartogh, "Feasibility of ultra-wideband SAW RFID tags meeting FCC rules" *IEEE Trans. Ultrasonics, Ferroelectric Freq. Control*, vol. 56, pp. 812-820, 2012.
16. F.J. Herraiz-Martínez, F. Paredes, G. Zamora, F. Martín, and J. Bonache, "Printed magnetoinductive-wave (MIW) delay lines for chipless RFID applications", *IEEE Trans. Ant. Propag.*, vol. 60, pp. 5075-5082, Nov. 2012.
17. S. Tedjini, E. Perret, A. Vena, D. Kaddout, "Mastering the electromagnetic signature of chipless RFID tags", in *Chipless and Conventional Radiofrequency Identification*, ed. IGI Global, 2012.
18. S. Preradovic, I. Balbin, N. C. Karmakar, and G. F. Swiegers, "Multiresonator-based chipless RFID system for low-cost item tracking," *IEEE Trans. Microw. Theory Techn.*, vol. 57, pp. 1411-1419, 2009.
19. S. Preradovic and N. C. Karmakar, "Design of chipless RFID tag for operation on flexible laminates," *IEEE Anten. Wireless Propag. Lett.*, vol. 9, pp. 207-210, 2010.
20. O. Rance, R. Siragusa, P. Lemaître-Auger, E. Perret, "Toward RCS magnitude level coding for chipless RFID," *IEEE Trans. Microw. Theory Techn.*, vol. 64, pp. 2315-2325, Jul. 2016.
21. J. McVay, A. Hoorfar, and N. Engheta, "Space-filling curve RFID tags," in Proc. of *2006 IEEE Radio Wireless Symp.*, pp. 199–202.
22. I. Jalaly and D. Robertson, "Capacitively-tuned split microstrip resonators for RFID barcodes," in Proc. of *European Microwave Conference*, October 2005, vol. 2, pp. 4–7.
23. H.-S. Jang, W.-G. Lim, K.-S. Oh, S.-M. Moon, and J.-W. Yu, "Design of low-cost chipless system using printable chipless tag with electromagnetic code", *IEEE Microw. Wireless Compon. Lett.*, vol. 20, pp. 640-642, 2010.
24. A. Vena, E. Perret, and S. Tedjini, "A fully printable chipless RFID tag with detuning correction technique", *IEEE Microw. Wireless Compon. Lett.*, vol. 22(4), pp. 209-211, 2012.
25. A. Vena, E. Perret, and S. Tedjini, "Design of compact and auto-compensated single-layer chipless RFID tag", *IEEE Trans. Microw. Theory Techn*., vol. 60(9), pp. 2913-2924, Sept. 2012.
26. A. Vena, E. Perret, and S. Tedjini, "High-capacity chipless RFID tag insensitive to the polarization", *IEEE Trans. Ant. Propag.*, vol. 60(10), pp. 4509-4515, Oct. 2012.
27. M. M. Khan, F. A. Tahir, M. F. Farooqui, A. Shamim, H. M. Cheema, "3.56-bits/cm^2 compact inkjet printed and application specific chipless RFID tag," IEEE Ant. Wireless Propag. Lett., vol. 15, pp. 1109-1112, 2016.
28. M. A. Islam and N. C. Karmakar, "A novel compact printable dual-polarized chipless RFID system," *IEEE Trans. Microw. Theory Techn.*, vol. 60, pp. 2142-2151, Jul. 2012.
29. R. Rezaiesarlak and M. Manteghi, "Complex-natural-resonance-based design of chipless RFID tag for high-density data," *IEEE Trans. Ant. Propag.*, vol. 62, pp. 898-904, Feb. 2014.
30. M. Svanda, J. Machac, M. Polivka, J. Havlicek., "A comparison of two ways to reducing the mutual coupling of chipless RFID tag scatterers," in Proc. of *21st International Conference on Microwave, Radar and Wireless Communications (MIKON)*, May 2016, pp. 1-4.
31. A. Vena, E. Perret, S. Tedjini, "Chipless RFID tag using hybrid coding technique," *IEEE Trans. Microw. Theory Techn.*, vol. 59, pp. 3356-3364, Dec. 2011.
32. A. Vena, E. Perret, S. Tedjini, "A compact chipless RFID tag using polarization diversity for encoding and sensing", *2012 IEEE Int. Conf. RFID*, pp. 191-197, 2012.
33. I. Balbin, N.C. Karmakar, "Phase-encoded chipless RFID transponder for large scale low cost applications", *IEEE Microw. Wireless. Comp. Lett.*, vol. 19, pp. 509-511, 2009.
34. S. Genovesi, F. Costa, A. Monorchio and G. Manara, "Chipless RFID tag exploiting multifrequency delta-phase quantization encoding", *IEEE Ant. Wireless, Propag. Lett.*, vol. 15, pp. 738-741, 2015.

35. C. Herrojo, J. Naqui, F. Paredes and F. Martín, "Spectral Signature Barcodes based on S-shaped Split Ring Resonators (S-SRR)", *EPJ Applied Metamaterials*, vol. 3, pp. 1-6, June 2016.
36. C. Herrojo, J. Naqui, F. Paredes, F. Martín, "Spectral signature barcodes implemented by multi-state multi-resonator circuits for chipless RFID tags", *IEEE MTT-S International Microwave Symposium* (IMS'16), San Francisco, May 2016.
37. C. Herrojo, F. Paredes, J. Mata-Contreras, S. Zuffanelli and F. Martín, "Multi-state multi-resonator spectral signature barcodes implemented by means of S-shaped Split Ring Resonators (S-SRR)", *IEEE Trans. Microw. Theory Techn.*, vol. 65, no. 7, pp. 2341-2352, July 2017.
38. C. Herrojo, J. Mata-Contreras, F. Paredes, F. Martín, "Near-Field chipless RFID encoders with sequential bit reading and high data capacity", *IEEE MTT-S Int. Microw. Symp*. (IMS'17), Honolulu, Hawaii, June 2017.
39. H. Chen, L. Ran, J. Huangfu, X. Zhang, K. Chen, T. M. Grzegorczyk, and J. A. Kong, "Left-handed materials composed of only S-shaped resonators," *Phys. Rev. E*, vol. 70, no. 5, p. 057605, Nov. 2004.
40. J. Naqui, J. Coromina, A. Karami-Horestani, C. Fumeaux, and F. Martín, "Angular displacement and velocity sensors based on coplanar waveguides (CPWs) loaded with S-shaped split ring resonator (S-SRR)", *Sensors*, vol. 15, pp. 9628-9650, 2015.
41. J. Mata-Contreras, C. Herrojo, and F. Martín, "Application of split ring resonator (SRR) loaded transmission lines to the design of angular displacement and velocity sensors for space applications", *IEEE Trans. Microw. Theory Techn.*, published online (doi: 10.1109/TMTT.2017.2693981).
42. C. Herrojo, J. Mata-Contreras, F. Paredes, F. Martín, "Microwave encoders for chipless RFID and angular velocity sensors based on S-shaped split ring resonators (S-SRRs)", *IEEE Sensors J*., vol. 17, no. 15, pp. 4805-4813, August 2017.